

Article

An Intelligent Controller Based on Extension Theory for Batteries Charging and Discharging Control

Kuei-Hsiang Chao ^{1,*}  and Jia-Yan Li ²¹ Department of Electrical Engineering, National Chin-Yi University of Technology, Taichung 41170, Taiwan² Prospective Technology of Electrical Engineering and Computer Science, National Chin-Yi University of Technology, Taichung 41170, Taiwan; as26393586@gmail.com

* Correspondence: chaokh@ncut.edu.tw; Tel.: +886-4-2392-4505 (ext. 7272); Fax: +886-4-2392-2156

Abstract: The main purpose of this paper is to develop an intelligent controller for the DC-link voltage of bidirectional soft-switching converters used in the batteries with equalizing charge and discharge control. To accelerate the equalizing charge and discharge speed of batteries, the DC-link voltage controller of the bidirectional converters is designed based on extension theory. Firstly, the photovoltaic module arrays (PVMAs) are used with the intelligent maximum power point tracker (MPPT) for supplying the power to the load side. Through the bidirectional soft-switching converters, the PVMAs will be allowed to carry out the uniform charging and discharging for the storage battery in order to achieve the intended energy storage and auxiliary power supply functions. In terms of the controller design, the quantitative design techniques are utilized, by which the P-I controller parameters will be designed for the converter when attempting to achieve the same control performance at different working points. As a next step, the aforesaid parameters are used together with the extenics theory. Based on the variation in the output power of the bidirectional converter and that in the voltage of the storage battery, it allows the system to find out the intended P-I controller parameters that will be approximate to the prescribed control performance when operating under different working conditions. As a result, the P-I controller will be provided with more efficient control flexibility and control performances. Finally, actual test results demonstrated that the response time of the proposed intelligent extension controller is shortened by 3% compared to the quantitative design of the proportional–integral (P-I) controller. Based on the proposed quantitative design of an intelligent controller for uniform charging and discharging management of batteries, the sustainable utilization of renewable sources of energy can be improved. At the same time, the better economic benefit of the energy preservation system is obtained. In addition, it also prolongs the life cycle of batteries, and then enhances the reliability of the batteries.

Keywords: intelligent controller; extension theory; bidirectional soft-switching converter; quantitative design; proportional–integral (P-I) controller



Citation: Chao, K.-H.; Li, J.-Y. An Intelligent Controller Based on Extension Theory for Batteries Charging and Discharging Control. *Sustainability* **2023**, *15*, 15664. <https://doi.org/10.3390/su152115664>

Academic Editor: Ashwin M. Khambadkone

Received: 5 September 2023

Revised: 23 October 2023

Accepted: 3 November 2023

Published: 6 November 2023



Copyright: © 2023 by the authors. Licensee MDPI, Basel, Switzerland. This article is an open access article distributed under the terms and conditions of the Creative Commons Attribution (CC BY) license (<https://creativecommons.org/licenses/by/4.0/>).

1. Introduction

The rapid growth of industry in recent years has led to a gradual shortage of electricity supply, resulting in high peak electricity bills [1]. To relieve the pressure of supplying electricity, it is essential to develop new and renewable sources of energy, and photovoltaic power is one of a few such main electricity sources. In addition, a photovoltaic power generation system is more flexible if combined with sustainable energy preservation methods, while the current main one is battery-based. Therefore, increasing importance of applications of sustainability has been attached to that research on energy preservation and release control methods of batteries. In particular, when multiple sets of batteries are used in series as a large energy preservation device, it is necessary to perform uniform charging and discharging control for series batteries in order to improve energy preservation

efficiency. In study [2], a structure for uniform battery charging and discharging was proposed, which controlled the DC-link voltage with a traditional proportional–integral (P-I) controller, achieving uniform battery charging and discharging. However, the response of the DC-link voltage control was slow, resulting in a slower uniform battery charging and discharging. In study [3], technology for lithium battery charging and discharging technology was proposed, which was mainly used in charging and discharging for electric vehicles (EVs) with two stages of constant voltage and constant current, achieving uniform battery charging and discharging. However, under different working conditions, it cannot quickly control the DC-link input voltage of the converter to a constant value, resulting in a slower uniform charging and discharging for series batteries. Although the voltage values of the batteries are not quoted in the distributed cooperative control mentioned in study [4], where uniform charging and discharging could be realized for multiple cells of series-connected batteries by applying the control algorithm, the state of charge (SOC) value of the charging and discharging should be set first for the aforesaid charging and discharging control and then the same SOC value shall be applied to the charging and discharging of all battery cells. When using this method to execute uniform charging and discharging for the batteries subjecting to higher SOC variations, it will bring about unnecessary energy loss. In study [5], an intelligent algorithm with faster calculation speed constructed with extension theory was developed, but advance training was required for higher control accuracy. In study [6], a P-I controller constructed with quantization design was proposed. At a selected operating point, optimal controller parameters could be designed according to preset control response performance, controlling the DC-link voltage to achieve preferred load regulation responses. In study [7], the parameters of the P-I controller could be adjusted automatically, but it was hard to achieve the fast response of control performance under different operating conditions. In literature [8–11], an intelligent controller was developed by combining fuzzy control with a P-I controller. However, fuzzy control was less flexible because the membership function of 0~1 was used to determine the intervals of operating conditions at a selected operating point, which affected the accuracy of its control. In study [12], poorer control response performance is observed when executing the quantitative design for the controller of the nonlinear systems. It is mainly because when executing the quantitative design, the parameters of the system model are remained in a fixed range so as to find out the most suitable controller parameters. In the nonlinear systems, however, the controller parameters acquired from the quantitative design should be retrieved from the fixed range. In this case, it may result in system instability once any working point or any system parameter has changed. Study [13] proposes that the parameters of a P-I controller can be determined directly according to the extenics theory. Although satisfactory control response performance can be achieved, it would be impossible to achieve the intended control performance from the deployed working points and it may even lead to system instability if excessive control efforts are applied. In order to solve the above problems, in this paper, the parameters of the P-I controller required for expected control response performance under different operating conditions are obtained by using quantization design technology. Then, with the extension theory applied, the correlation degree of $-1\sim 1$ is used to determine the intervals of operating conditions at a selected operating point, so that preferred controller parameters are available. As a result, when the battery charging and discharging is controlled under different operating points, preferred response performance is achieved with the control of the DC-link voltage of the converter.

In this paper, Section 2 mainly introduces the architecture of the energy storage system that will be configured by combining the photovoltaic generation system with the storage battery system. Section 3 explains the design process and method for the DC-link voltage controller, including the execution of quantitative design for the P-I controller parameters according to the prescribed control performance of the system. As a next step, it will be used with the extenics theory for selecting the appropriate P-I controller parameters so that the DC-link voltage of the bidirectional converters will be controlled when operating in

different working conditions so as to obtain the intended control performance. Finally, the operation result will be measured in Section 4 so as to verify the feasibility of the designed intelligent controller. As a final step, conclusions will be made in Section 5 in order to explain the research directions in the future.

2. Energy Storage System Structure of Photovoltaic Power System

The main purpose of this paper is to explain the DC-link smart voltage controller designed for the bidirectional voltage buck-boost soft-switching converters in order to stabilize the DC-link voltage so that the uniform charging and discharging will be achieved more quickly for multiple sets of batteries that are configured in the series-connection type. In the meantime, it will also be used with the photovoltaic power generation system and the storage battery for realizing energy storage and auxiliary power supply, as per the overall architecture indicated in Figure 1. Because the output power of the PVMA will change along with the sunshine amount, the boost converter is used together with the MPPT [14] so as to maintain its output power at the maximum power point. In the aspect of the selected uniform charging/discharging architecture, it is composed of several groups of bidirectional buck-boost soft-switching converters that are configured in the series-connection type [2]. The PVMA utilizes the sensing circuit for transmitting the voltage and the current generated with the maximum power tracker and the uniform charging/discharging circuit back to the TMS320F2809 digital signal processor for carrying out the computation. In the meantime, a set of uniform charging/discharging rules are also established for limiting the battery from outputting the maximum charging/discharging current so as to prevent the excessive current from damaging the battery and to verify the feasibility of the tested uniform charging/discharging architecture. Finally, the extenics theory is also utilized to carry out the quantitative design of the parameters required for the bidirectional buck-boost soft-switching converters so that the output voltage response of these converters will achieve the intended performance. In addition, the resulting charging/discharging speed is compared with the P-I controller using the parameters designed with the conventional quantitative method in order to demonstrate its excellent charging/discharging response performance.

The MPPT techniques [14–17] are mainly developed to allow the PVMA to demonstrate the MPPT under a variety of conditions in different working environments so as to enhance the conversion efficiency of the PVMA. The MPPT method selected in this paper is configured according to the improved artificial bee colony algorithm [14]. The aforesaid algorithm is included in the essay published by the author of study [14] previously.

In order to combine batteries with the photovoltaic power generation system for controlling energy storage and release, a bidirectional buck-boost soft-switching converter [2,18] is selected in this paper for controlling energy storage and release. The low-voltage side of this bidirectional converter is connected to the battery, while the high-voltage side is connected to the DC-link capacitor at the output of the MPPT of the PVMA [2].

When uneven charging and discharging is caused due to different power levels of batteries connected in series, it can automatically adjust the current levels of charging and discharging, achieving uniform battery charging and discharging. A structure for control of uniform charging and discharging is proposed by the authors of [2], which can independently charge and discharge each battery connected in series, achieving uniform charging and discharging quickly. This structure not only could effectively limit the current levels of charging and discharging, but also slows down battery aging. Figure 1 is an energy storage system structure for a photovoltaic power generation system combined with uniform charge and discharge control [2]. This structure uses a digital signal processor (DSP) TMS320F2809 as its control core [2] and sends the voltage and current signals detected with sensors to the digital signal processor for calculation. This allows control of the uniform charging and discharging controller, control of signals with corresponding pulse width modulation (PWM) output, control of conducting time switched using the

power semiconductor of the converter, adjustment of the charging and discharging current levels of each battery, and for achieving uniform battery charging and discharging control quickly. However, during the control of uniform battery charging and discharging, it is important to maintain the constant DC-link voltage at the input of the converter. As a result, the design and control performance of the DC-link voltage controller will greatly affect the time achieving uniform battery charging and discharging. Indicated in Figure 1 is the overall system architecture, and the specifications of the single piece photovoltaic module are listed in Table 1. In such modules, the four in series and three in parallel connection are utilized to create the 500 W PVMA. By combining the specifications of bidirectional soft-switching converters listed in Table 2, it allows the system to execute the battery charging and discharging control.

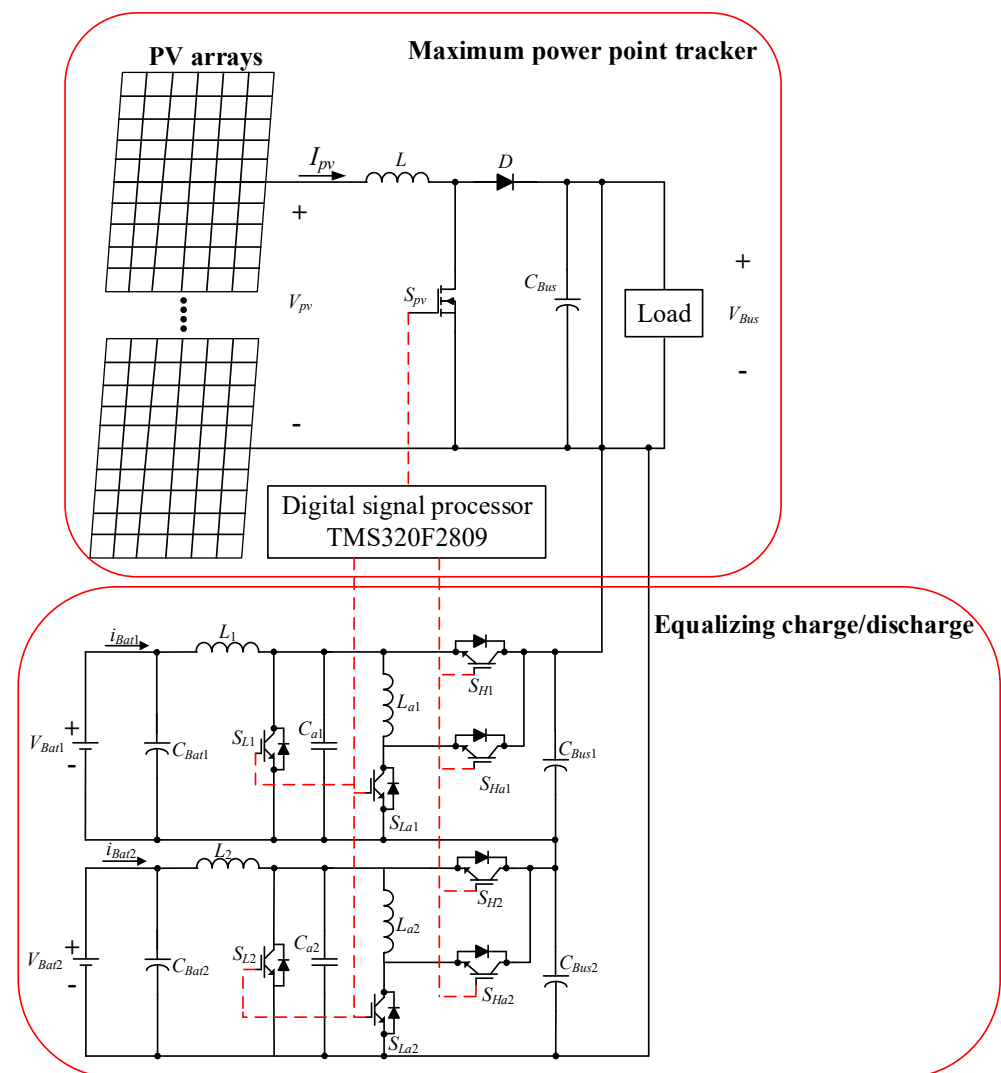


Figure 1. An energy storage system structure for photovoltaic power generation system combined with uniform charge and discharge control.

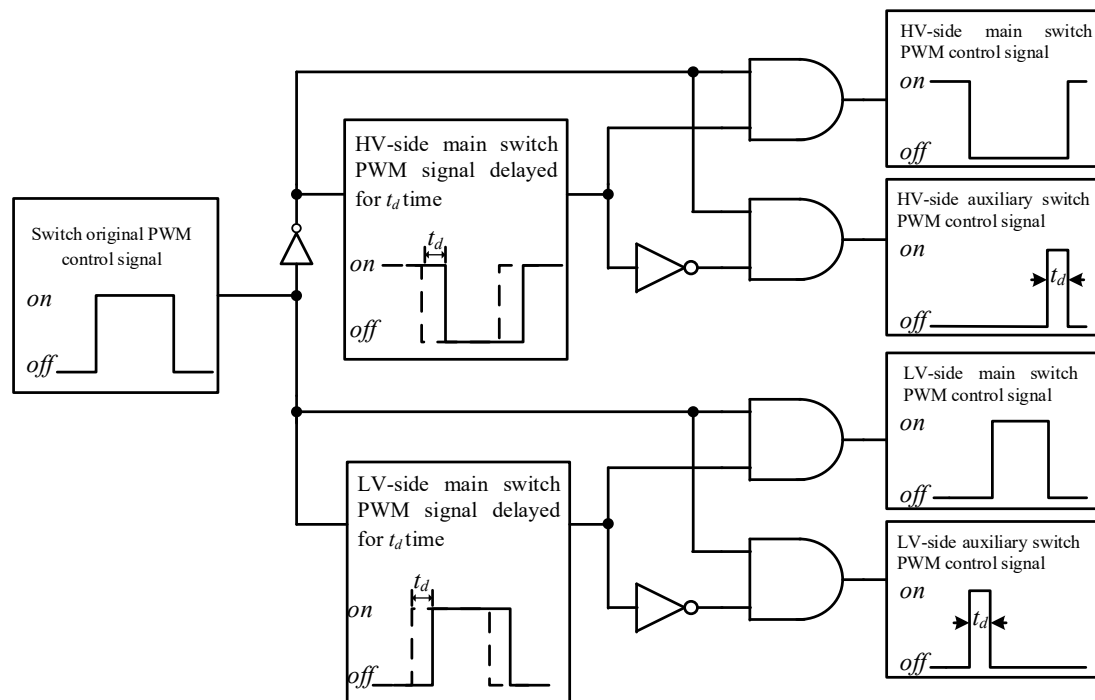
Table 1. Specifications of the single piece for SUM SWM-50 W PV module.

Maximum Power (P_{max})	50 W
Voltage at P_{max} (V_{mp})	18.18 V
Current at P_{max} (I_{mp})	2.75 A
Open-circuit voltage (V_{oc})	22.32 V
Short-circuit current (I_{sc})	2.89 A

Table 2. Specifications of bidirectional soft-switching converters.

Voltage (V_{Bus}) of high voltage (HV) side (DC-link)	240 V
Voltage (V_{Bat1}) of low voltage (LV) side battery #1	24 V
Voltage (V_{Bat2}) of LV side battery #2	24 V
Switching frequency (f)	50 kHz
Maximum output power (P_{max})	300 W
Voltage ripple of HV side	0.5%
Voltage ripple of LV side	0.5%

In Figure 1, the lower side is the circuit diagram of the bidirectional soft-switching converters in which the resonance circuit is composed of auxiliary switch S_{La1} (S_{La2}), resonance capacitor C_{a1} (C_{a2}), and the back-connected diode of S_{H1} (S_{H2}) and S_{Ha1} (S_{Ha2}). Figure 2 explains the PWM signal triggering process for the auxiliary switch being deployed in the resonance circuit. Through Figure 2, it can be learned that the original triggering signal of the main switch S_{L1} (S_{L2}) will be postponed for a certain period (t_d) and then energized through auxiliary switch S_{La1} (S_{La2}). In this way, the resonance loop of the auxiliary circuit is created through the resonance capacitor C_{a1} (C_{a2}) and inductor L_{a1} (L_{a2}), thus allowing the main switch to achieve zero voltage switching (ZVS) [2,18].

**Figure 2.** PWM signal triggering flow schematic view of auxiliary switch in resonance branch [2].

Listed in Table 3 are the specifications of each component in the boost converter designed for tracking the maximum power. Listed in Table 4 are the specifications of each component in the bidirectional soft-switching converters designed for executing the battery charging and discharging control in which the resonance capacitances (C_{a1} and C_{a2}) are replaced with the IGBT-based parasitic capacitance (45 pF).

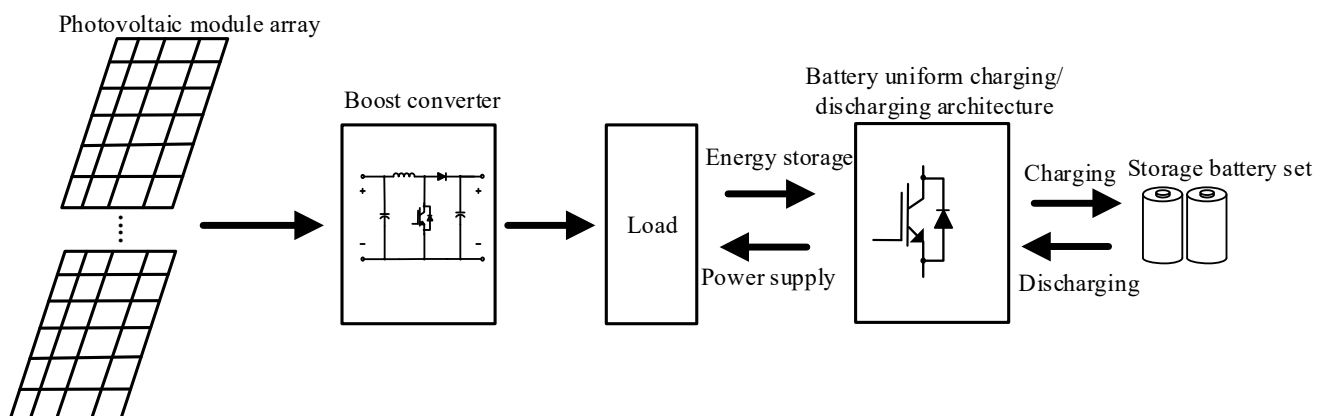
Table 3. Component specifications of boost converters.

Component Name	Energy Storage Inductor (L)	Filter Capacitor (C_{Bus})	Switch (S_{PV}) IRFP460	Diode (D) FMP-G5FS
Specification	1.152 mH	390 μ F/450 V	500 V/20 A	1500 V/10 A

Table 4. Component specifications of bidirectional soft-switching converters.

Component	Value
Main inductors (L_1 and L_2)	1.425 mH
LV-side capacitors (C_{Bat1} and C_{Bat2})	330 μ F/450 V
HV-side capacitors (C_{Bus1} and C_{Bus2})	330 μ F/450 V
Main switches (S_{L1} and S_{L2})	IGBT IXGH40N120C3D1 (75 A/1200 V)
Auxiliary switches (S_{La1} and S_{La2})	IGBT IGP30N65H5XKSA1 (55 A/650 V)
Resonance inductors (L_{a1} and L_{a2})	22 μ H
Resonance capacitors (C_{a1} and C_{a2})	45 pF/650 V

In this paper, the quantitative design will be executed for the intelligent controller using the DC-link voltage supplied with the bidirectional buck-boost soft-switching converters [2,18], and the designed controller parameters allow the battery to achieve the uniform charging and discharging more quickly. In the meantime, it is also used with the photovoltaic generation system for the battery to utilize the energy storage and the auxiliary power supply functions so as to stabilize the DC-link voltage. Indicated in Figure 3 is its overall architectural process. Because the output power of the PVMA will change along with the sunshine amount, the boost converter should be used with the artificial bee colony algorithm [14] so as to maintain its output power at the maximum output point. In the aspect of the uniform charging/discharging architecture used in this paper, it is composed of several sets of bidirectional buck-boost soft-switching converters [2,18] that are configured in the series-connection type. These converters are equipped with the sensing circuit for transmitting the voltage and the current of the MPPT and the uniform charging/discharging circuit back to the TMS320F2809 digital signal processor [2] for carrying out the computation. In addition, a set of uniform charging/discharging rules are also established for limiting the battery from outputting the maximum charging/discharging current in order to prevent the excessive current from damaging the battery and to verify the feasibility of the selected uniform charging/discharging architecture in controlling the stability of the DC-link voltage. Finally, the extenics theory is also utilized to select better P-I controller parameters for the quantitatively designed bidirectional buck-boost soft-switching converters so that the DC-link voltage response of the converter may achieve the intended performance when operating in different working conditions. In the meantime, it will be used for comparing with the control performance of the conventional quantitative P-I controller.

**Figure 3.** Battery energy storage system architectural process by combining with PVMA and battery uniform charging/discharging control [2].

3. Design of DC-Link Voltage Controller

This paper is focusing on the load regulating performance designed for controlling the DC-link voltage of the bidirectional converters. The impact of the load characteristic variations to the control performance of the P-I controller being designed according to the

conventional quantitative method has been considered at the current stage. In the next stage, the aforesaid control performance will be used for comparing with other controllers according to the intelligent rules and the intelligent online regulating parameters designed for the conventional P-I controller. Its purpose is to propose the controller that will be designed with higher robustness.

The bidirectional soft-switching converters are controlled with the dual-loop control method in which the outer loop is controlled with the DC-link voltage and the inner one is controlled with the uniform charging/discharging current supplied with the storage battery. In this regard, the detailed control method is described in the essay previously published by the author and it is also included in [2]. Therefore, it will not be repeatedly described in this paper.

Based on the specifications of the bidirectional soft-switching converters indicated in Table 2, the 240 V voltage (V_{Bus}) of the HV side refers to the value of DC-link voltage. Traditional P-I controllers usually have preferred control performance only at their operating points and obtain their parameters through trial and error. In order to obtain the parameters of the P-I controller required for preset control performance under a certain operating point, quantization design technology is required [19]. In recent years, many intelligent algorithms have been proposed [4–13]. Although they can change those control parameters under different operating conditions to achieve preferred load regulation responses, most of these algorithms are too complicated to implement. Therefore, a P-I controller constructed with extension theory combined with quantization design is proposed in this paper to form an intelligent controller, thereby solving those difficulties for implementation.

3.1. Parameters of P-I Controller Constructed with Quantization Design

In study [20], the control block diagram of the voltage loop with the bidirectional buck-boost soft-switching converter shown in Figure 1 was obtained, as shown in Figure 4. In Figure 4, $G_{cv}(s)$ is a voltage controller, $G_p(s)$ is the transfer function of the bidirectional buck-boost soft-switching converter, K_{pv} is the voltage conversion coefficient when the DC-link power is disturbed, and K_v is the voltage sensing conversion factor with a value of 0.01.

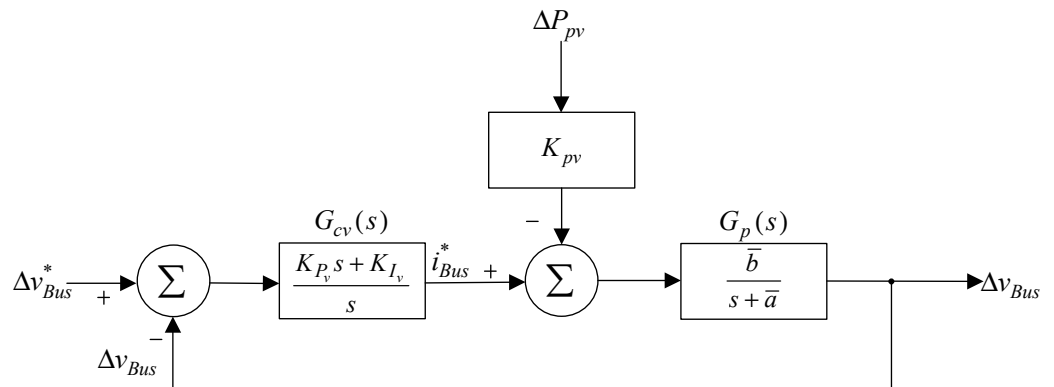


Figure 4. The control block diagram of voltage loop with the bidirectional buck-boost soft-switching converter.

According to the control block diagram shown in Figure 4, the transfer functions of Δv_{Bus} vs. Δv_{Bus}^* and Δv_{Bus} vs. ΔP_{pv} can be derived as Equations (1) and (2), respectively.

$$H_v(s) = \left. \frac{\Delta v_{Bus}}{\Delta v_{Bus}^*} \right|_{\Delta P_{pv}=0} = \frac{bG_{cv}K_v}{s+a+bG_{cv}K_v} \triangleq \frac{c_1}{s+r} \quad (1)$$

$$H_p(s) = \left. \frac{\Delta v_{Bus}}{\Delta P_{pv}} \right|_{\Delta v_{Bus}^*=0} = \frac{-bK_{pv}K_v}{s+a+bG_{cv}K_v} \triangleq -\frac{c_2}{s+r} \quad (2)$$

By using the step response method [21], $a = 26.88$ and $b = 537.7$ can be estimated using Equations (1) and (2), and the transfer function $G_p(s)$ of a bidirectional buck-boost soft-switching converter can be derived as Equation (3).

$$G_p(s) = \frac{b}{s+a} = \frac{537.7}{s+26.88} \quad (3)$$

In order to make the step response of the system with characteristics of no overshoot, zero steady-state error, fast voltage recovery time, and small drop of maximum voltage, Equations (4) and (5) can be obtained as the specifications of the maximum voltage drop $\hat{v}_{Bus,max}$ and recovery time t_r selected.

$$f_1(u_1, u_2) = \hat{v}_{Bus,max} - \frac{K_{pv}\bar{b}\Delta P_{pv}}{u_1 - u_2} \left[e^{\frac{-u_1}{u_1-u_2} \ln(\frac{u_1}{u_2})} - e^{\frac{-u_2}{u_1-u_2} \ln(\frac{u_1}{u_2})} \right] \quad (4)$$

$$f_2(u_1, u_2) = 0.05\hat{v}_{Bus,max} - \frac{K_{pv}\bar{b}\Delta P_{pv}}{u_1 - u_2} [e^{-u_1 t_r} - e^{-u_2 t_r}] \quad (5)$$

By using Matlab2020a software, the variables of Equations (4) and (5), the two nonlinear equations, can be calculated, and parameters K_P and K_I of the voltage controller can be derived as Equations (6) and (7), respectively.

$$K_P = \frac{(u_1 + u_2) - \bar{a}}{\bar{b}} \quad (6)$$

$$K_I = \frac{u_1 u_2}{\bar{b}} \quad (7)$$

3.2. Extension Theory

To achieve uniform battery charging and discharging quickly, the extension theory [22–25] was used in this paper to select different controller parameters at different operating points, achieving preferred response performance of DC-link voltage. First, the parameters of a P-I controller required for desired control performance under different operating conditions are obtained with quantization design; next, the operating mode at the current operating point is determined with extension theory; the correlation degree was calculated based on features of the selected operating point to determine the required parameters of the P-I controller; as a result, the best parameters of the P-I controller are obtained accordingly. In the extension theory, matter–affair is expressed as matter–elements shown in Equation (8), where R is the basic element that describes matter–affair, i.e., matter–element, and N , C , and V are the three elements that constitute the matter–element, i.e., N for the name of matter–affair, C for the feature of matter–affair, and V for the feature value of matter–affair. And the matter–element model is shown as Equation (9), where C is the characteristic of F , V_p is the characteristic value of C , i.e., classical domain, and g expresses five operating modes. In the extension theory, controller parameters under various operating conditions need to be included in the matter element model, and the weighting value is selected to represent the importance of each parameter.

$$R = (N, C, V) \quad (8)$$

$$R_g = (F, C, V_p) = \begin{bmatrix} F & C_1 & \langle x_1, y_1 \rangle \\ & C_2 & \langle x_2, y_2 \rangle \end{bmatrix}, g = 1, 2, \dots, 5 \quad (9)$$

The extension distance, which is the distance relationship between one certain point on the physical domain to one interval, is expressed as a function like Equation (10).

$$\varphi(f, F_0) = \left| f - \frac{v_a + v_b}{2} \right| - \frac{v_b - v_a}{2} \quad (10)$$

In addition to the correlation between one point and one interval, the relationships between one point and two intervals or one interval and another interval must also be considered. Therefore, if $F_0 = \langle V_a, V_b \rangle, F = \langle V_c, V_d \rangle$ are inside two intervals of the physical domain, respectively, while interval F_0 is inside the interval F , the rank value of the point f to interval F_0 and the rank value of two intervals F can be expressed as Equation (11).

$$D(f, F_0, F) = \begin{cases} \varphi(f, F) - \varphi(f, F_0), & f \notin F_0 \\ -1 & , f \in F_0 \end{cases} \quad (11)$$

As a result, the correlation function equals to the distance divided by the function of the rank value, as shown in Equation (12).

$$K(f) = \frac{\varphi(f, F_0)}{D(f, F_0, F)} \quad (12)$$

In the case of $f = (V_a + V_b)/2$, the correlation function has a maximum value, which is called elementary correlation function, its schematic diagram being shown in Figure 5. In addition, in the case of $K(f) < -1$, the point f is outside the interval F ; in the case of $K_f > 0$, the point f is inside the interval F_0 ; and in the case of $-1 < K(f) < 0$, the point f is inside the extension domain.

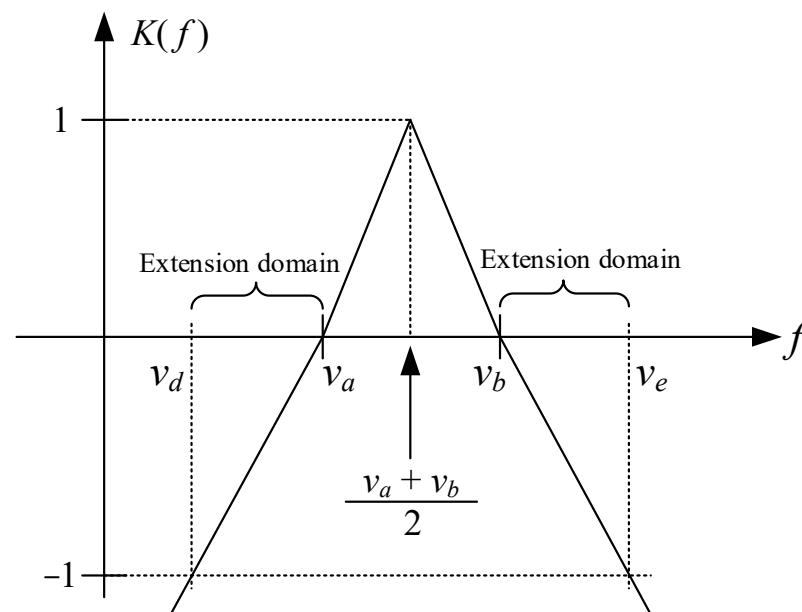


Figure 5. Schematic diagram of elementary correlation function.

3.3. Proposed P-I Controller Constructed with Extension Theory Combined with Quantization Design

In this paper, the parameters of a P-I controller required under different operating conditions are determined with extension theory. Mainly with the quantization design method applied and based on the control performance (maximum voltage drop $\hat{v}_{Bus,max} = 1V/W$, i.e., $100 W \rightarrow 100 V$; voltage recovery time $t_r = 0.7 s$) of desired DC-line voltage at different operating points, the required parameters of a P-I controller are calculated accordingly. First, the output power change and battery voltage change are set as characteristic values with the extension theory, and the range of the neighborhood domain is set, as shown in Table 5. Next, the ranges of the classical domain at different operating points from Mode 1 to Mode 5 are set with values among the range of the neighborhood domain, as shown in Table 6. Finally, Equations (10)–(12) are used to calculate those correlation functions, which are classified as different working modes using characteristics; then, Equation (13) is used to calculate the correlation degree of each operating mode type according to the importance of each characteristic to obtain the optimal operating mode under current operating

conditions; the optimal parameters of a P-I controller constructed with quantization design in the corresponding operating mode type are obtained accordingly; as a result, preferred response performance of DC-link voltage is achieved and preferred response performance of DC-link voltage, and required time for uniform battery charging and discharging, is shortened.

$$\lambda_g = \sum_{j=1}^2 W_j K_{gj}, g = 1, 2, \dots, 5 \quad (13)$$

Table 5. Neighborhood domain of DC-link voltage control constructed with extension theory.

Feature	Range of Neighborhood Domain
Output power change	−150 W~150 W
Battery voltage change	−1 V~1 V

Table 6. Classical domain of each characteristic under different operating modes constructed with extension theory.

Type	Characteristic	Output Power Change
	Mode 1	150 W > X > 20 W
	Mode 2	150 W < X
	Mode 3	−20 W < X < 20 W
	Mode 4	−150 W < X < −20 W
	Mode 5	−150 W > X

With the variation range allowed for varied output power and storage battery voltage ratings being established for the bidirectional converters, multiple sets of P-I controller parameters are designed through the offline quantitative method according to the prescribed load regulation control performance (as per Table 7). Next, the online measuring is conducted for learning about the level of the variations between the following two features, i.e., the output power of bidirectional converters and the voltage of the storage battery. Through the intelligent algorithm of the extenics theory, the most suitable P-I controller parameters are selected for controlling the bidirectional converter so that its DC-link voltage will be approximate to the prescribed load regulation response when the varied level of output power and storage battery voltage is changing. In view of this, the P-I controller parameters selected for the online operation described in this paper are not the optimal control parameters; instead, the P-I controller parameters approximate to the prescribed control performance are selected.

Table 7. Corresponding P-I controller parameters under Mode 1 in the classical domain constructed with extension theory.

Output Power Change	Battery Voltage Change	Output Value
150 W < X < 70 W	−1.0 V > X > −0.5 V	$K_P = 0.285, K_I = 3.35$
120 W < X < 60 W	−1.0 V > X > −0.5 V	$K_P = 0.28, K_I = 3.38$
80 W < X < 50 W	−0.9 V > X > −0.4 V	$K_P = 0.275, K_I = 3.41$
70 W < X < 40 W	−0.8 V > X > −0.3 V	$K_P = 0.27, K_I = 3.44$
60 W < X < 40 W	−0.7 V > X > −0.3 V	$K_P = 0.265, K_I = 3.47$
50 W < X < 30 W	−0.7 V > X > −0.2 V	$K_P = 0.26, K_I = 3.50$
40 W < X < 30 W	−0.5 V > X > −0.2 V	$K_P = 0.255, K_I = 3.53$
30 W < X < 20 W	−0.5 V > X > −0.2 V	$K_P = 0.25, K_I = 3.56$

Table 7 shows the parameters of the quantized P-I controller ($K_P = 0.25, K_I = 3.56$) at the operating point (DC-link voltage $v_{Bus} = 180$ V and load $P = 500$ W) of Mode 1 in

the classical domain constructed with extension theory, where the values of K_P and K_I are the parameters calculated with Equations (6) and (7). Based on the parameters at this operating point, the output power change of Mode 1 is divided into several ranges, and those parameters are assigned as different controller parameters according to corresponding ranges of output power and battery voltage change. The values of K_P and K_I for other operating modes can be obtained in the same way.

Table 8 shows the characteristic weight values of the DC-link voltage controller constructed with extension theory. Those weight values are used to measure the importance of various characteristics, allowing more accurate controller parameters calculated by means of extension theory accordingly. The DC-link voltage change is greatly affected by the output power change in the converter, but less affected by the battery voltage change. Therefore, as the weight values of the two characteristics are set to 0.65 and 0.35, respectively, the correlation degree can be obtained through Equation (13), the calculation equation of the extension method, accurately achieving the preferred K_P and K_I , the parameters of a P-I controller based on the level of the correlation degree.

Table 8. The weights of DC-link voltage control constructed with extension theory.

Characteristic	Weights
Output power change	0.65
Battery voltage change	0.35

As a next step, the output power of the bidirectional converter and the variation of the storage battery voltage required for the online measuring are referenced in Equation (13) for calculating the correlation degree between the categories listed in Table 7. As a final step, the P-I controller parameters (K_P and K_I) pertaining to the category that is presenting the tightest correlation degree are selected as the increment of the controller.

4. Test Results

Indicated in Figure 6 is the outlook appearance of the overall hardware testing device. Figure 7a,b are a comparison of testing results from P-I DC-link voltage controllers constructed with extension theory and quantitative design, which show their performance with 50 W power loading and curtailing, respectively. As seen in Figure 7a, it takes 0.5 s for recovering DC-link voltage with 50 W loading, and another 0.5 s for recovering with 50 W curtailing. On the other hand, for the testing result from the DC-link voltage P-I controller constructed with extension theory with 50 W power loading and curtailing, as seen in Figure 7b, it only takes 0.15 s for recovering DC-link voltage with 50 W loading, and another 0.15 s for recovering with 50 W curtailing. Based on the comparison of testing results, the following is seen: faster recovery time of DC-link voltage from the DC-link voltage controller constructed with extension theory than the one constructed with quantization design with 50 W power loading or curtailing, respectively.

Figure 8a,b are a comparison of testing results from P-I DC-link voltage controllers constructed with extension theory and quantitative design, which show their performance with 100 W power loading and curtailing, respectively. As seen in Figure 8a, it takes 0.8 s for recovering DC-link voltage with 100 W loading, and another 0.9 s for recovering with 100 W curtailing. On the other hand, for the testing result from the DC-link voltage controller constructed with extension theory with 100 W power loading and curtailing, as seen in Figure 8b, it only takes 0.2 s for recovering DC-link voltage with 100 W loading, and another 0.3 s for recovering with 100 W curtailing. Based on the comparison of testing results, the following is seen: faster recovery time of DC-link voltage from the DC-link voltage P-I controller constructed with extension theory than the one constructed with quantization design with 100 W power loading or curtailing, respectively.

Figure 9a,b are a comparison of testing results from P-I DC-link voltage controllers constructed with extension theory and quantitative design, which show their performance with 150 W power loading and curtailing, respectively. As seen in Figure 9a, it takes

1.5 s for recovering DC-link voltage with 150 W loading, and another 1.2 s for recovering with 150 W curtailing. On the other hand, for the testing result from the DC-link voltage controller constructed with extension theory with 150 W power loading and curtailing, as seen in Figure 9b, it only takes 0.9 s for recovering DC-link voltage with 150 W loading, and another 0.7 s for recovering with 150 W curtailing. Based on the comparison of testing results, the following is seen: faster recovery time of DC-link voltage from the DC-link voltage P-I controller constructed with extension theory than the one constructed with quantization design with 150 W power loading or curtailing, respectively.

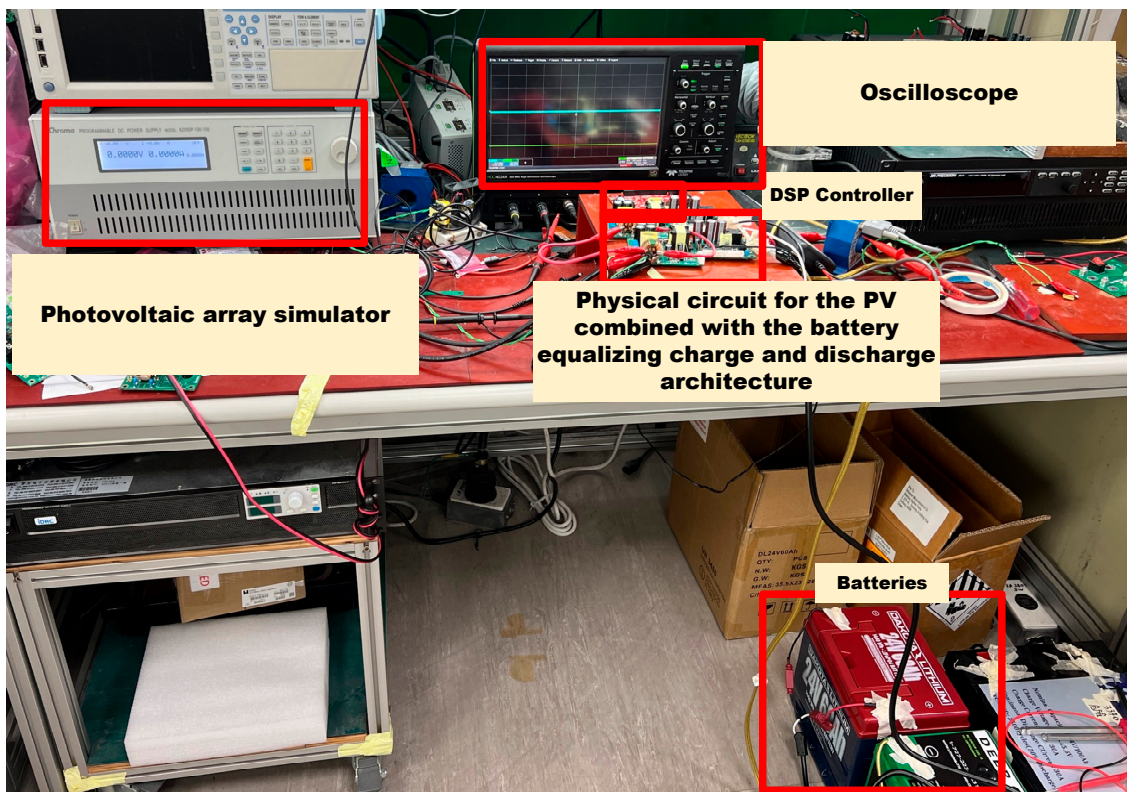


Figure 6. Outlook appearance of the overall hardware testing device.

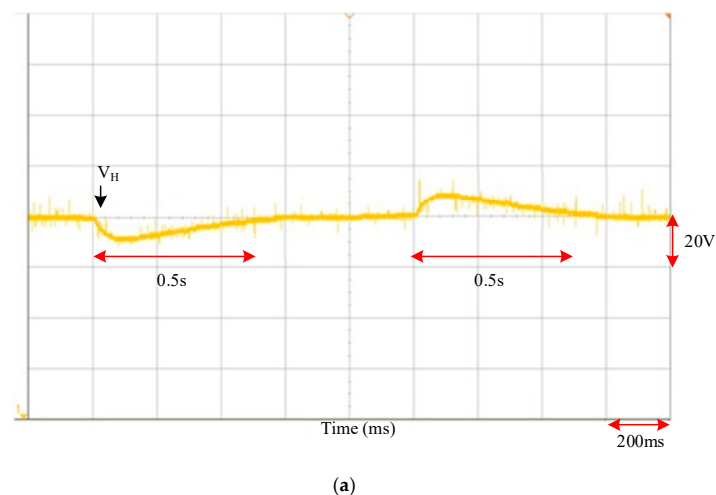


Figure 7. Cont.

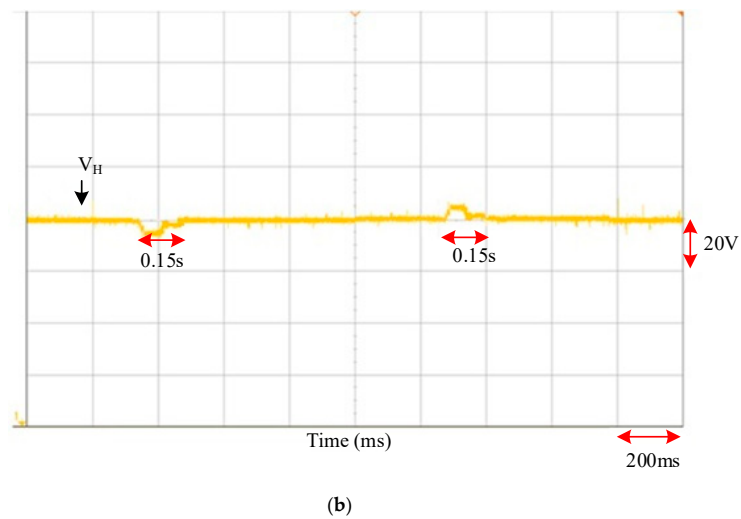


Figure 7. The comparison of testing results from uniform charging and discharging controllers with 50 W power loading and curtailing: (a) P-I controller constructed with quantization design; (b) P-I controller constructed with extension theory combined with quantitative design.

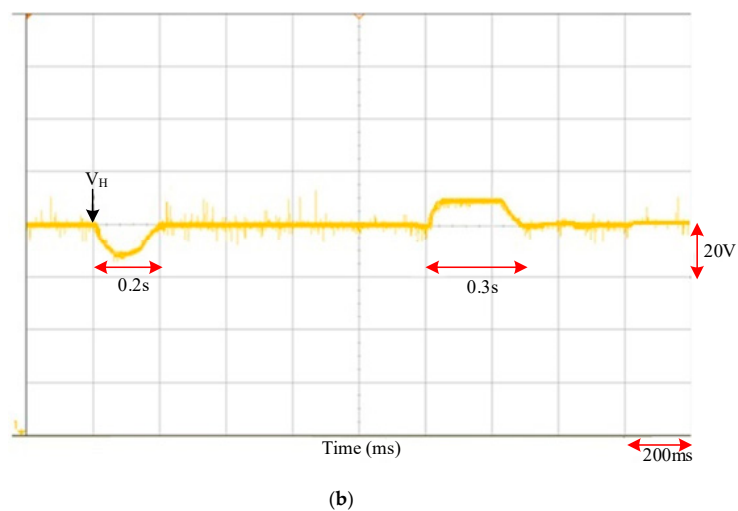
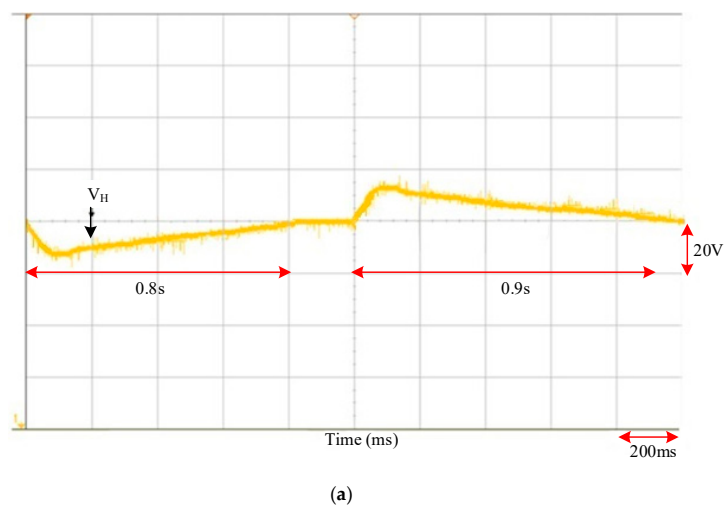


Figure 8. The comparison of testing results from uniform charging and discharging controllers with 100 W power loading and curtailing: (a) P-I controller constructed with quantization design; (b) P-I controller constructed with extension theory combined with quantitative design.

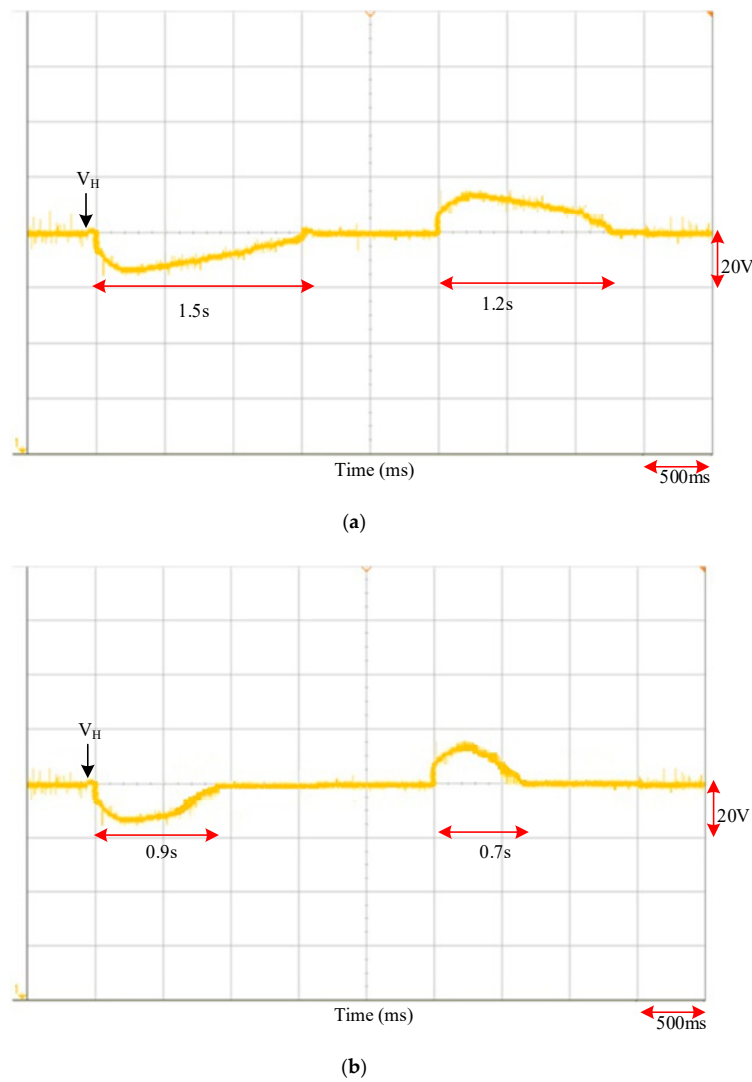


Figure 9. The comparison of testing results from uniform charging and discharging controllers with 150 W power loading and curtailing: (a) P-I controller constructed with quantization design; (b) P-I controller constructed with extension theory combined with quantitative design.

Table 9 shows the recovery time of the DC-link voltage for two controllers under different power changes. As seen in this table, it shows better recovery time of DC-link voltage from the intelligent DC-link voltage controller constructed with extension theory than the one constructed with quantization design at any operating point.

Table 9. Comparison of recovery time of DC-link voltage from different controllers at different operating points.

Power Change (ΔP)	Controller Type	P-I Controller Constructed with Extensive Theory Combined with Quantization Design		P-I Controller Constructed Only with Quantization Design	
		Power Loading	Power Curtailing	Power Loading	Power Curtailing
50 W		0.15 s	0.15 s	0.5 s	0.5 s
100 W		0.2 s	0.3 s	0.8 s	0.9 s
150 W		0.9 s	0.7 s	1.5 s	1.2 s

Indicated in Figures 7–9 is the speed response of the designed intelligent controller that is provided with quicker restoration function for the controlled DC-link voltage. It is learned that during the charging and discharging process, the battery is also designed with faster

uniform charging/discharging speed. In this regard, the waveform response required for the storage battery charging/discharging current and the uniform charging/discharging is described in the essay previously published by the author and it is also included in study [2]. Therefore, it will not be repeatedly described in this paper.

At the current stage, the control performance was tested under different working conditions for the intelligent control being developed by combining the extenics theory and the quantitatively designed P-I controller that are mentioned in this paper. The measured result defined in Figures 7–9 proves that it has better control performance than the P-I controller designed according to the conventional quantitative method [19]. In the meantime, Figure 9 also indicates that when using the PVMAs designed with 500 W of rated output power and when 150 W of output power variation is observed in the bidirectional converter, it will be regarded as one of the cases where extreme changing of the output power has occurred to the PVMAs. To prevent the variation level higher than 150 W from causing excessive output control force to the P-I controller, the 150 W controller parameters will be used for regulating the DC-link voltage beforehand and then the controller parameters are adjusted until the variation of the bidirectional converter is lower than 150 W. In this way, the system damage can be avoided as may be caused by the excessive variation value when instantaneous error exists in the power sensing value or when the system is interfered with by the intensified noise. For this reason, the intelligent controller proposed in this paper will be equipped with excellent reliability. In the next stage, the aforesaid control performance will be used for comparing with other controllers according to the intelligent rules and the worst-case working conditions where the conventional P-I controller is used for carrying out the intelligent online parameter regulating. Its purpose is to propose the controller that will be designed with higher robustness and higher reliability.

In design, the load required for this system will be supplied alternately using the photovoltaic generation system and the storage battery. If the load is increased to the extent that PVMAs are no longer able to supply adequate electric energy, then it will lead to the dropping of the DC-link voltage. In this case, the battery will discharge the electricity for carrying out the auxiliary power supply so as to maintain the intended DC-link voltage value. If the load is too high thus that the system fails to maintain the fixed value for the DC-link voltage and where it has dropped to the minimal voltage rating required for the storage battery to maintain the power supply, then it means that the storage battery is unable to supply the auxiliary power continuously. In this case, the system will stop supplying the power to prevent the entire system and the load from damage. During practical applications, the system will set up appropriate capacity for the PVMAs according to the level of the load and will also execute the mixed power supply by using reasonable capacity of the storage battery.

The main purpose of this paper is to improve the defect where the quantitatively designed P-I controller currently used is not provided with the required robustness. Therefore, the extenics theory is proposed for combining the aforesaid quantitatively designed P-I controller in order to overcome the defect where intended control performance cannot be achieved with the P-I controller parameters being designed for the specific working point, as will be caused by the change in the working point in the system. At the current stage, therefore, the controller performance will be compared with the conventional P-I controller being designed through the quantitative method. In the next stage, the control performance will be compared with the controller according to the intelligent rules and the intelligent online regulating parameters designed for the conventional P-I controller so as to propose the controller designed with more intensified robustness.

5. Conclusions

A DC-link voltage intelligent controller with a converter constructed with extension theory combined with quantization design is proposed in this paper, and corresponding P-I controller parameters under different mode types at different operating points are

calculated with extension theory. Operating modes are classified into five types, and the most preferred parameters K_P and K_I of the P-I controller are calculated through the quantization design method according to the expected control performance. Based on the comparison of testing results, the following is seen: faster recovery time of DC-link voltage from the DC-link voltage controller constructed with extension theory than the one constructed with quantization design either with 50 W, 100 W, or 150 W power loading or curtailing, respectively. Due to the quantization design technology applied, it is possible to calculate the different parameters of the P-I controller required for the same control performance of the converter at different operating points in advance. Moreover, with extension theory combined, it is also possible to derive the parameters of the P-I controller required for expected similar control performance under different operating condition points based on the output power change in the converter and battery voltage change. This allows such controllers to have higher control flexibility and performance. When it is used in the structure for uniform battery charging and discharging, quicker uniform battery charging and discharging can be achieved.

The energy storage system is combined with a photovoltaic power generation system and batteries. The proposed uniform charge/discharge control strategy can improve the life cycle and energy management efficiency for batteries, and then elevate the sustainable utilization of renewable sources of energy. Therefore, this paper proposes a safe and reliable management method for a sustainable energy preservation system. However, the selected uniform charging/discharging architecture can only be used for measuring the voltage and the current of the battery and for determining whether the battery charging and discharging level is balanced or not. Therefore, the stage of charge (SOC) and the state of health (SOH) are not added in the measuring test. Therefore, it would be impossible to confirm the charge and health status of the battery. For this reason, the battery management system (BMS) should be established for future research programs as to enhance the servicing efficiency of the battery and extend the battery life.

Author Contributions: K.-H.C. planned, wrote, edited, and reviewed the project. J.-Y.L. was responsible for designing the bidirectional soft-switching converters and DC-link voltage controller to be used in the batteries with equalizing charge and discharge control. K.-H.C. manages the project. All authors have read and agreed to the published version of the manuscript.

Funding: The authors gratefully acknowledge the support and funding of this project by National Science and Technology Council, Taiwan, under the Grant Number NSTC-112-2221-E-167-002.

Institutional Review Board Statement: Not applicable.

Informed Consent Statement: Not applicable.

Data Availability Statement: This study did not report any data.

Conflicts of Interest: The authors of the manuscript declare no conflict of interest.

References

1. Taipower—Understanding Tariffs. Available online: <https://www.taipower.com.tw/tc/page.aspx?mid=213&cid=352&cchk=52452a93-48e7-47ab-9cd3-b0c6836cf15e> (accessed on 20 April 2023).
2. Chao, K.H.; Huang, B.Z.; Jian, J.J. An Energy Storage System Composed of Photovoltaic Arrays and Batteries with Uniform Charge/Discharge. *Energies* **2022**, *15*, 8–2883. [CrossRef]
3. Malla, A.B.; Myneni, H. Analysis of Different Charging methods of Batteries for EV Applications with Charge Equalization. In Proceedings of the 2023 IEEE IAS Global Conference on Renewable Energy and Hydrogen Technologies, Male, Maldives, 11–12 March 2023; pp. 1–6.
4. Shipeng, L.; Yunlong, S.; Bin, D.; Guicheng, C.; Qi, Z.; Chenghui, Z. A State-of-Charge Uniformity Control Method for Energy Storage Batteries Based on Distributed Cooperative Control. In Proceedings of the 2021 China Automation Congress, Beijing, China, 22–24 October 2021; pp. 1–5.
5. Yang, F.; Zhang, C.A. Classification Model Based on Extenics with Weighted Reatures for Rolling Bearing Quality Test. In Proceedings of the 2011 Second International Conference on Mechanic Automation and Control Engineering, Hohhot, China, 15–17 July 2011; pp. 3760–3762.

6. Karthik, R.; Hari, A.S.; Pavan Kumar, Y.V.; Pradeep, D.J. Modelling and Control Design for Variable Speed Wind Turbine Energy System. In Proceedings of the 2020 International Conference on Artificial Intelligence and Signal Processing (AISP), Amaravati, India, 10–12 January 2020; pp. 1–6.
7. Yumuk, E.; Copot, C.; Ionescu, C.M. A Robust Auto-Turning P-I Controller Design Based on S-Shaped Time Domain Respinse. In Proceedings of the 2022 8th International Conference on Control Decision and Information Technologies, Istanbul, Turkey, 17–20 May 2022; pp. 525–530.
8. Shi, J.Z. A Fractional Order General Type-2 Fuzzy P-I Controller Design Algorithm. *IEEE Access* **2020**, *8*, 52151–52172. [[CrossRef](#)]
9. Bambulkar, R.R.; Phadke, G.S.; Salunkhe, S. Movement Control of Robot Using Fuzzy PID Algorithm. In Proceedings of the 3rd International Conference on Electrical, Electronics, Engineering Trends, Communication, Optimization and Sciences (EEECOS), Tadepalligudem, India, 1–2 June 2016; pp. 1–5.
10. Ma, F. An Improved Fuzzy P-I Control Algorithm Applied in Liquid Mixing System. In Proceedings of the 2014 IEEE International Conference on Information and Automation, Hailar, China, 28–30 July 2014; pp. 587–591.
11. Dehghani, A.; Khodadadi, H. Designing a Neuro-Fuzzy PID Controller Based on Smith Predictor for Heating System. In Proceedings of the 2017 17th International Conference on Control, Automation and Systems, Jeju, Republic of Korea, 18–21 October 2017; pp. 15–20.
12. Pan, T.T.; Chang, X.H.; Lui, Y. Robust Fuzzy Feedback Control for Nonlinear Systems with Input Quantization. *IEEE Trans. Fuzzy Syst.* **2022**, *30*, 4905–4914. [[CrossRef](#)]
13. Wu, J. Stability Theory for Infinite-Dimensional Linear Systems Based on An Extension Method. *IMA J. Math. Control. Inf.* **1998**, *15*, 117–132. [[CrossRef](#)]
14. Sundareswaran, K.; Sankar, P.; Nayak, P.S.R.; Simon, S.P.; Palani, S. Enhanced Energy Output from a PV System under Partial Shaded Conditions through Artificial Bee Colony. *IEEE Trans. Energy Convers.* **2014**, *6*, 198–209. [[CrossRef](#)]
15. Yuan, B.; Lai, X.; Ye, Q.; Li, Y. Ramp-Based Soft-Start Circuit with Soft-Recovery for DC-DC Buck Converters. In Proceedings of the IEEE International Conference on Electron Devices and Solid-State Circuits, Hong Kong, China, 3–5 June 2013; pp. 1–2.
16. Ram, J.P.; Pillai, D.S.; Rajasekar, N.; Stachan, S.M. Detection and Identification of Global Maximum Power Point Operation in Solar PV Applications Using a Hybrid ELPSO-P&O Tracking Technique. *IEEE Trans. Emerg. Sel. Top. Power Electron.* **2020**, *8*, 1361–1374.
17. Badoud, A.E. Real-Time Experimental Analysis of Hybrid BG-FL Based MPPT Controller for a Photovoltaic System under Partial Shading Conditions. In Proceedings of the 2022 19th International Multi-Conference on Systems, Signals & Devices (SSD), Sétif, Algeria, 6–10 May 2022; pp. 1409–1414.
18. Lee, I.H.; Kim, J.G.; Lee, T.G.; Jung, Y.C.; Won, C.Y. A New Bidirectional DC-DC Converter with ZVT Switching. In Proceedings of the 2012 IEEE Vehicle Power and Propulsion Conference, Seoul, Republic of Korea; 2012; pp. 684–689.
19. Chao, K.H.; Huang, B.Z. Quantitative Design for the Battery Equalizing Charge/Discharge Controller of the Photovoltaic Energy Storage System. *Batteries* **2022**, *8*, 278. [[CrossRef](#)]
20. Angelo, R.M.; Io, A.K.; Almeida, M.P.; Silveria, R.G.; Oilveria, R.G. OntoQSAR: An Ontology for Interpreting Chemical and Biological Data in Quantitative Structure-Activity Relationship Studies. In Proceedings of the 2020 IEEE 14th International Conference on Semantic Computing, San Diego, CA, USA, 3–5 February 2020; pp. 203–206.
21. Zhou, L. Quantitative E-Business System Design Method. In Proceedings of the 2015 IEEE 12th International Conference on e-Business Engineering, Beijing, China, 23–25 October 2015; pp. 1–8.
22. Wang, M.H.; Lu, S.D.; Huang, M.L.; Hsieh, C.C.; Wei, S.E. Hybrid Methodology Based on Extension Theory for Partial Discharge Fault Diagnosis of Power Capacitors. *IEICE Electron. Express* **2020**, *17*, 20200250. [[CrossRef](#)]
23. Xu, H.; Li, Q.; Su, J.; Yan, L. Integration of Information Models for Industrial Internet Based on Extenics. In Proceedings of the 2020 IEEE 5th International Symposium on Smart and Wireless Systems within the Conferences on Intelligent Data Acquisition and Advanced Computing Systems, Dortmund, Germany, 17–18 September 2020; pp. 1–6.
24. Ma, Z.; Lang, K.; Zhang, Y.; Xing, S. Comprehensive Evaluation of Emergency Situation after Collisions at Sea Based on Extenics. In Proceedings of the 2021 IEEE 4th Advanced Information Management, Communicates, Electronic and Automation Control Conferences, Chongqing, China, 18–20 June 2021; pp. 2042–2048.
25. Sun, Y.; Yuan, T.; Chen, J.; Feng, R. Chinese Sign Language Key Action Recognition Based on Extenics Immune Neural Network. In Proceedings of the 2020 IEEE International Conference on Advances in Electrical Engineering and Computer Applications, Dalian, China, 25–27 August 2020; pp. 187–191.

Disclaimer/Publisher's Note: The statements, opinions and data contained in all publications are solely those of the individual author(s) and contributor(s) and not of MDPI and/or the editor(s). MDPI and/or the editor(s) disclaim responsibility for any injury to people or property resulting from any ideas, methods, instructions or products referred to in the content.